

Acoustic phonon transmission and thermal conductance in a three-stub quantum waveguide

Jian-Hua Zhang*

Department of Physics, Xiangnan University, Chenzhou 423000, China

Received 21 October 2010; Accepted (in revised version) 14 November 2010

Published Online 17 January 2011

Abstract. Using the scattering matrix method, we investigate the acoustic phonon transmission and thermal conductance in a quantum waveguide with three stubs at low temperature. It is found that transmission coefficient shows periodic feature and the number of cutoff frequency bands increases with increasing of height h ; and the thermal conductance exhibits oscillatory decaying behavior with increasing of the widths between any two stubs; In addition, thermal conductance is sensitive to the width and height of stubs; The results show that changing the geometric parameters of the stubs could provide an efficient way to control the thermal conductance of the proposed micro-structures artificially.

PACS: 63.22.+m, 73.23.Ad, 44.10.+i

Key words: T-shaped quantum waveguide, scattering matrix method, acoustic transmission coefficient, thermal conductance

1 Introduction

Acoustic phonon heat transmission in a quantum waveguide structure is a very important subject and has attracted increasing attention in recent years [1–10]. The characters of phonon transmission and thermal conductance are mainly researched objects because phonon transmission and thermal conductance are two vital parameters in semiconductor nanostructure which plays a key role in controlling the performance and stability of phonon device. Many theoretical and experimental investigations of phonon transport in various kinds of nanostructure such as thin films [2], quantum wells [3], superlattices [4], nanowires [5–7], one-dimensional glass [8], and nanotubes [9, 10] have been reported and made tremendous progress in the last decade. Using the Landauer formulation of transport theory, several groups [11–14] have derived the expressions of phonon transmission and thermal conductance for ballistic phonon transport at a low enough temperature in an ideal elastic beam

*Corresponding author. *Email address:* zhangjianhua6846991@126.com (J. H. Zhang)

and found that the thermal conductance which quantized in a universal value $\pi^2\kappa_B T/3h$, analogous to the well-known $2e^2/h$ electronic conductance quantum. And they also found that thermal conductance is controlled by the first several modes at low temperature. These predictions have been verified experimentally by Schwab *et al.* [15]. Li and his copartner researched phonon transmission and thermal conductance in a quantum waveguide structure by using the scattering matrix method recently, then they revealed a series of interesting characters such as acoustic phonon mode splitting behavior [16] and the nonintegral quantized thermal conductance of an asymmetric y -branch three terminal junction [17] at very low temperatures through a T-shaped quantum waveguide. Scattering matrix method is an effective method for accounting of phonon or electron transmission and thermal conductance in nanostructure. Using this method, in this paper, we mainly investigate the characters of phonon transmission and thermal conductance in a three-stub quantum waveguide structure and obtain some novel and interesting physical characteristics which are different from other shaped discontinuity quantum waveguide nanostructure. For example, transmission coefficient shows periodic feature with the increasing of heights h at the different reduced frequencies and thermal conductance exhibits oscillatory decaying behavior with the width between any two stubs.

2 Model and formalism

We consider the geometric structure as shown in Fig. 1, which is divided into seven regions (I-VII). We assume that the temperature in region ξ is T_ξ and the temperature difference δT is very small, so the mean temperature (T) can be adopted as the temperature of every region in the following calculations. As we known if the thickness of structure is very thin, then we can ignore mode mixing effects at boundaries and interfaces. In really three-dimensional case, then the thickness should be small with respect to the other dimensions and also to the wavelength of the elastic waves. There is no mixing of the Z mode, so we only need calculate a two-dimensional case.

We employ the expression of thermal conductance K as [18, 19]

$$K = \frac{\hbar^2}{k_B T^2} \sum_m \frac{1}{2\pi} \int_{\omega_m}^{\infty} \tau_m(\omega) \frac{\omega^2 e^{\beta\hbar\omega}}{(e^{\beta\hbar\omega})^2} d\omega, \quad (1)$$

where $\tau_m(\omega)$ is the energy transmission coefficient form mode m of region I at frequency ω across all the interfaces into the modes of region VII, ω_m is the cutoff frequency of the m -th mode, $\beta = 1/k_B T$, k_B is the Boltzman constant, T is the temperature and \hbar is the Plank's constant. The effect of scattering is introduced through the transmission coefficient, so the central issue in predicting the thermal conductance is then to calculate the transmission coefficient. When waveguide structure is continuous, $\tau_m(\omega) = 1$, but if the structure is discontinuity, $\tau_m(\omega) \leq 1$, owing to scattering effect in the stubs.

In this paper, we employ the elastic model to calculate the transmission coefficient of acoustic phonon. To our knowledge, there are three different modes in quantum waveguide

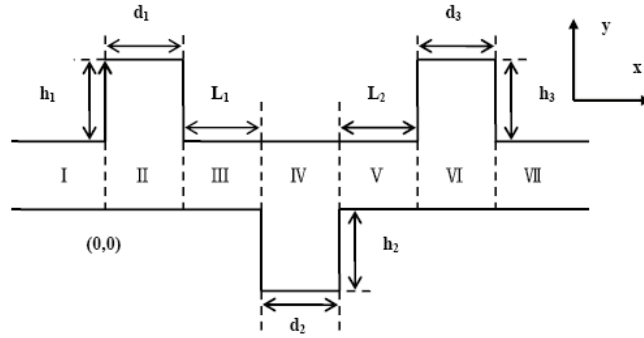


Figure 1: Three T-shaped quantum waveguide: two main quantum wires with three finite stubs which is divided into seven regions(I-VII), those regions' transverse dimensions are $W_I, W_{II}, W_{III}, W_{IV}, W_V, W_{VI}$ and W_{VII} respectively. The other parameters are shown in the figure.

structure, here we only investigate SH mode propagating in the x direction. Also it should be pointed that we only calculate in the stress-free boundary condition, for it is more useful than hard-wall boundary condition in practice.

The displacement field function satisfies the scalar potential equation,

$$\frac{\partial^2 u}{\partial t^2} - v_{SH}^2 \nabla^2 u = 0, \tag{2}$$

where the SH wave velocity v_{SH} is related to the mass density ρ and elastic stiffness constant C_{44} ,

$$v_{SH} = \sqrt{C_{44}/\rho}. \tag{3}$$

The stress-free boundary condition at the edges requires that $\hat{n} \cdot \nabla u = 0$, with \hat{n} the normal to the edge. The phonon displacement field equations in region ξ can be written in the form

$$\mu^\xi(x, y) = \sum_{m=0}^N \left(g_m^\xi e^{ik_m^\xi(x-x_\xi)} + h_m^\xi e^{-ik_m^\xi(x-x_\xi)} \right) \phi_m^\xi(y), \tag{4}$$

where x_ξ is the reference coordinate along the x direction for region ξ , g_ξ and h_ξ are constants to be determined by matching the boundary conditions. $\phi_m^\xi(y)$ ($\xi = I, II, III, IV, V, VI$ and VII) represents the orthogonal transverse mode m in region ξ ,

$$\phi_m^\xi(y) = \begin{cases} \sqrt{\frac{2}{W_\xi}} \cos \frac{n\pi}{W_\xi} y, & m \neq 0, \\ \sqrt{\frac{1}{W_\xi}}, & m = 0, \end{cases} \tag{5}$$

k_m^ξ can be expressed in terms of incident phonon frequency ω , the SH wave velocity μ_{SH} , and the transverse dimension W_ξ of region ξ by the energy conservation condition

$$k_m^{\xi 2} = \frac{\omega^2}{\mu_{SH}^2} - \frac{m^2 \pi^2}{W_\xi^2}. \quad (6)$$

In principle, the sum over m in above equations includes all propagating modes and evanescent modes. However, in the real calculations, we take into account all the propagating modes and several lowest evanescent modes to meet the desired precision. In the calculates, we will employ those values of dielectric constants and mass density of GaAs referred to [20]: $C_{44}(\text{GaAs})=5.99(10^{10}\text{Nm}^{-2})$ and $\rho(\text{GaAs})=5317.6(\text{kg}\cdot\text{m}^{-3})$.

3 Numerical results and discussion

We first research transmission coefficient dependence on the height of the stub and the incident phonon reduced frequency ω/Δ in the structure, as shown in Fig. 2. Here, we choose $W_I = W_{III} = W_{IV} = W_{VII} = 10\text{nm}$, $L_1 = L_2 = 10\text{ nm}$, $d_1 = d_2 = d_3 = 10\text{ nm}$. From Fig. 2, we can clearly see that

- 1) total transmission coefficient is always unity with any incident phonon reduced frequency when $h=0$. This is because the stubs vanish and the structure reverts to being a straight quantum waveguide for this case, there is no imperfect coupling and ballistic transport through the structure;
- 2) as $\omega \rightarrow 0$, total transmission coefficient approaches unity and is independent of the height of the stub, unlike the case of electrical transport, where the transmission is always close to zero when the Fermi energy approaches zero. The reasons for these phenomena are that acoustic phonon satisfies the stress-free boundary condition, whereas the electron satisfies the grid boundary condition. The stress-free boundary condition allows the propagation of acoustic phonon when $\omega \rightarrow 0$, the wavelength of phonon is much larger than the dimension of the scattering region, the displacement field becomes essentially the same throughout. As can be seen in Fig. 2, the transmission coefficient presents periodic character as a function of the heights of the stubs and period length decrease with an increase in the reduced frequency. This is related to the conditions of stationary wave and we will illuminate this issue in detail in Fig. 3.

To comprehend the characters of phonon transmission as a function of the heights of the stubs more clearly, we give its two-dimensional pictures as shown in Fig. 3. Here, we explore phonon transmission for (i): $h_1 = h_2 = h_3 = h$; (ii): $h_1 = h_3 = h = 10\text{ nm}$, $h_2 = h$; (iii): $h_1 = h_2 = 10\text{ nm}$, $h_3 = h$. First, the transmission exhibits a periodic pattern as a function of h for a given frequency, and the number of the period decreases with an increase in the reduced frequency. This is related to the conditions of stationary wave. It is known that there are incident wave and the reflected wave in the waveguide which interfere with each other and form stationary

wave. When the phase shift between them equals to $2n\pi$, the transmission will be reinforced and when the phase shift is $(2n+1)\pi$, the transmission will be zero, and thus a periodic oscillation appears in the transmission spectra as the figure described. As can be seen in Fig. 3, the periods are same for a given reduced frequency whatever the heights of the stubs are. For example, there are six periods when $\omega/\Delta=1$ and four periods when $\omega/\Delta=0.6$. The phenomena indicate that the period of transmission coefficient is dependent on the reduced frequency and is independent of the heights of stubs. The transmission coefficients are always unity in Fig. 3(a) when $h=0$ for the reduced frequency, as it is aforementioned. However, it is clearly seen from Fig. 2(b) and Fig. 2(c) that transmission coefficients for fixing h_1 and h_3 and increasing h_2 are different from those for fixing h_1 and h_2 and increasing h_3 at certain frequency. This is owing to the fact that the orthogonal transverse modes in the second stub are different from those in the third stub.

To investigate the properties of phonon transmission as a function of reduced frequency ω/Δ , we give its two-dimensional results as shown in Fig. 4. From Fig. 4, we can see clearly that the phonon transmission approaches unity when $\omega \rightarrow 0$, as it is mentioned in Fig. 2. Transmission spectra present a series of peaks and valleys with increasing the height of the stub and cutoff frequency bands at which all phonons are reflected completely are clearly observed in Fig. 4. Further calculations show that the number of cutoff frequency bands depends on the heights of the stubs. And the higher the stub, the more the cutoff frequency bands. For example, there is only one cutoff frequency band when the heights of the stubs are 2 nm, whereas there are four cutoff frequency bands when the heights of the stubs are 40 nm in Fig. 3(a). Moreover, the cutoff frequency bands shift to a lower reduced frequency ω/Δ with increasing heights of the stubs. This is owing to the fact that the total reflection

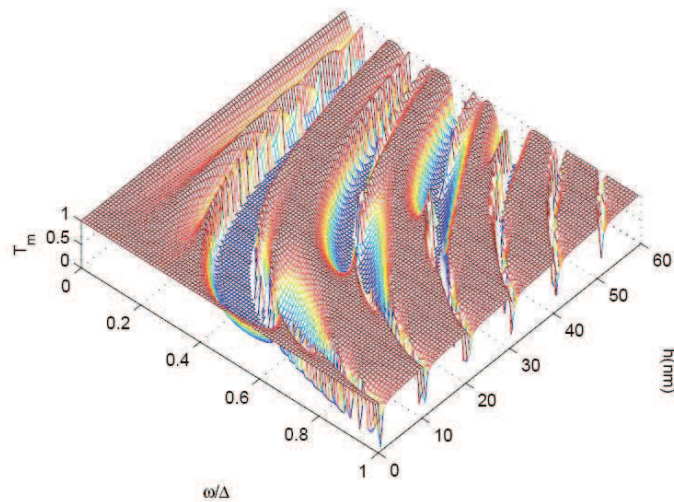


Figure 2: Transmission coefficient versus the height h and the incident phonon reduced frequency ω/Δ . Here, $h_1=h_2=h_3=h$.

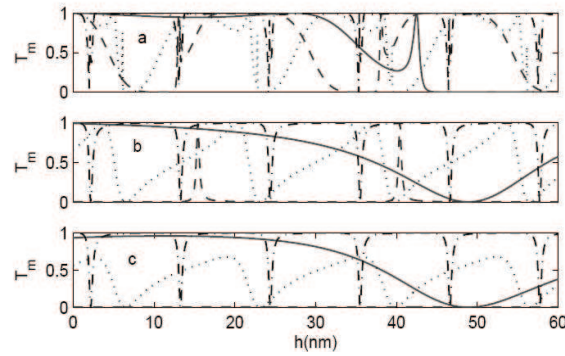


Figure 3: Transmission coefficient as a function of the height h for different reduced frequencies: (a) for $h_1=h_2=h_3=h$; (b) for $h_1=h_3=h=10$ nm, $h_2=h$; (c) for $h_1=h_2=10$ nm, $h_3=h$. The solid, dashed, dotted and dash-dotted curves are for $\omega/\Delta=0.1,0.4,0.6,0.9$, respectively.

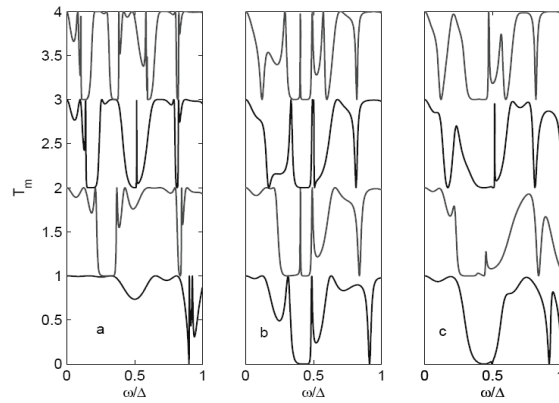


Figure 4: Total transmission coefficient as a function of the reduced frequency ω/Δ of incident phonons at the different heights h . (a) for $h_1=h_2=h_3=h$ and curves from below to above correspond to the height $h=2$ nm, 15 nm, 28 nm, 40 nm. (b) for $h_1=h_3=h=10$ nm, $h_2=h$ and curves from below to above correspond to the height $h=2$ nm, 15 nm, 28 nm, 40 nm. (c) for $h_1=h_2=10$ nm, $h_3=h$ and curves from below to above correspond to the height $h=2,10,28,40$ nm.

is controlled by the coupling strength of the propagating lowest-order modes and the excited modes in regions *II*, *IV* and *VI*. It is known that the coupling strength can be expressed by the overlap of the transverse functions of the incident wave and the excited wave: $Q_{mn} = \int \phi_m^I(y)\phi_n^{II}(y)dy$ [21], where m and n are indices of the transverse modes in regions *I* and *II*, respectively. Also, the case is the same for regions *III* and *IV*, as well as regions *V* and *IV*. So, with the increasing of the height h , excited modes will interfere with propagation modes in regions *II*, *IV* and *VI* and coupling strength will be enhanced.

Next, we turn to study the characters of thermal conductance in the structure. Here, $h_1 = h_2 = h_3 = h$, $d_1 = d_2 = d_3 = d$. For the structure discussed here, the stress-free boundary condition is also applied. Fig. 5 shows the thermal conductance divided by temperature K/T , which is reduced by the zero temperature the ideal universal value $\pi^2 k_B^2 / 3h$, as a function of the parameter h for different temperatures with all of modes. We find that reduced thermal conductance is close to the ideal universal value, $\pi^2 k_B^2 / 3h$, when $h \rightarrow 0$ at a very low temperature. This is owing to the fact that the stubs vanish and the structure reverts to being a uniform waveguide, in which no scattering happens in the whole quantum waveguide, and only zero mode can be excited. Thus only the zero mode contributes to the thermal conductivity and the conductivity of zero mode is close to the ideal universal value in such a uniform waveguide at a very low temperature, as shown in Fig. 5. It is worth pointing out that the conductivity of zero mode first decreases and then increase with an increase in temperature. Here, we only discuss the characters of thermal conductance when temperature is 0.0522 K and 0.1739 K. When $h \rightarrow 0$, the thermal conductance at $T = 0.1739$ K is larger than that at $T = 0.0522$ K, and the higher temperature is, the larger thermal conductance will be. This is because the higher transverse modes $m(m > 0)$ are excited and these modes splice bring the increase of thermal conductance at the higher temperature. We also show thermal conductance is always large at the beginning but quickly decline with the increasing heights h whatever width d is. The result shows that when the parameter h is very small the wavelength of phonon is larger than the width of stubs so that the effect of stubs' scattering is not very large, but scattering and coupling are rapidly strengthened with an increase in height h . Thermal conductance linearly decreases with the increasing height h when $T = 0.0522$ K, however, thermal conductance will first decrease and then oscillate with the increasing height h when $T = 0.1739$ K, as shown in Fig. 5.

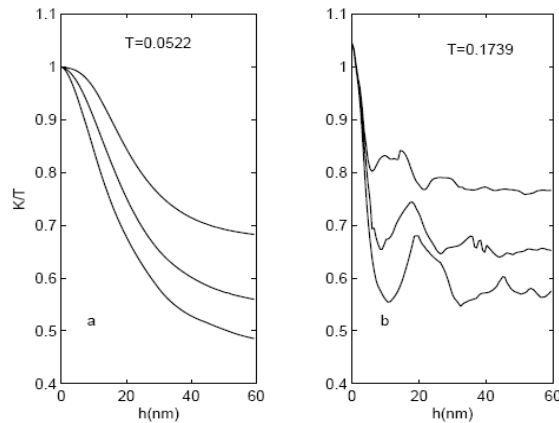


Figure 5: The thermal conductance K/T as a function of the height h for different temperatures and different widths d ; (a) correspond to the reduced temperature $T = 0.0522$ K; (b) correspond to the reduced temperature $T = 0.1739$ K. Curves from below to above correspond to the width $d = 15$ nm, 10 nm, 5 nm. Here, $L_1 = L_2$.

Finally, we turn to discuss the effects of length between two stubs on the thermal conductance (shown in Fig. 6). We first elucidate the characters of the total thermal conductance with the length L for different heights of stubs and different temperatures. Some main characters can be seen from the picture. First, when the structural parameters of the stubs are all utterly same, we find that the total thermal conductance in Fig. 6(a) is larger than those in Fig. 6(b). It means that total thermal conductance is different for different temperatures. This originates from the higher the temperature, the more the modes in the quantum waveguide, and they affect each other, and so, the total thermal conductance is different. Then, it is clearly observed that the total thermal conductance decreases with the increasing of the heights h whenever the temperature is 0.0522 K or 0.1739 K. This is because the effect of phonon scattering by the stubs is reinforced with the increasing of the heights of stubs which leads to the decrease in the phonon transmission. Now, we elucidate Figs. 6(a) and 6(b), respectively. From Fig. 6(a), it can be clearly seen that the total thermal conductance increases until L is 7 nm and then decreases to a certain value and keeps its size with the increasing of L when the temperature is 0.0522 K. However, the total thermal conductance presents oscillatory decaying behaviors with the increase in the width L when the temperature is 0.1739 K. This indicates that the thermal conductance of zero mode is sensitive to the total thermal conductance. When temperature is very low, only zero mode exists in the quantum waveguide. The higher the temperature, the more mode in the quantum waveguide and the more complex mode-mode coupling. And when length L is larger enough, the mode-mode coupling becomes very weak, and the thermal conductance will keeps a certain value. So L is vital to the total thermal conductance and we can control the total thermal conductance by changing L in the design of devices.

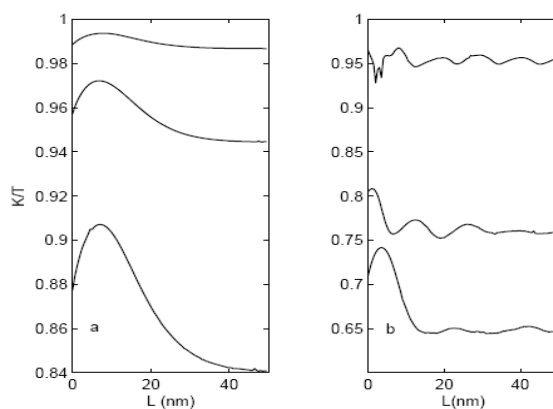


Figure 6: The thermal conductance K/T as a function of the length L for different temperatures and different heights h ; (a) correspond to the reduced temperature $T=0.0522$ K; (b) correspond to the reduced temperature $T=0.1739$ K. Curves from below to above correspond to the height $h=10$ nm, 5 nm and 2 nm. Here, $L_1=L_2=L$.

4 Summary

In conclusion, we have presented numerical calculations of the phonon transmission and thermal conductivity in a dielectric quantum waveguide structure at the stress-free boundary condition in this paper. We mainly research on the relationship between phonon transmission and thermal conductance and quantum structure parameters in a three-stub quantum waveguide. The results show some interesting physical effects: transmission coefficient shows periodic feature and the number and location of cutoff frequency bands have great changes with the increasing of heights h ; The thermal conductance exhibits oscillatory decaying behaviors with increasing the width between any two stubs; The transmission coefficient and thermal conductance is sensitive to the width and height of stub; From these results it is expected that by designing the structural parameters in dielectric quantum waveguide one can control the transmission spectrum and thermal conductance of the proposed structure to match practical requirements in devices.

Acknowledgment. This work was supported by the Scientific Research Fund of Hunan Provincial Education Department under Grant No. 09C920.

References

- [1] J. D. Lu, L. Shao, and Y. L. Hou, *Chinese Phys. Lett.* 24 (2007) 793.
- [2] W. Liu and M. Asheghi, *Appl. Phys. Lett.* 84 (2004) 3819.
- [3] A. Balandin and K. L. Wang, *Phys. Rev. B* 58 (1998) 1544.
- [4] M. V. Simkin and G. D. Mahan, *Phys. Rev. Lett.* 84 (2000) 927.
- [5] X. Lü, J. H. Chu, and W. Z. Shen, *J. Appl. Phys.* 93 (2003) 1219.
- [6] W. Q. Huang, K. Q. Chen, and Z. Shuai, *Int. J. Mod. Phys. B* 19 (2005) 1017.
- [7] Y. M. Zhang, C. H. Xu, and S. J. Xiong, *Chinese Phys. Lett.* 24 (2007) 1017.
- [8] D. M. Leitner, *Phys. Rev. B* 64 (2001) 094201.
- [9] P. Kim, L. Shi, A. Majumdar, and P. L. McEuen, *Phys. Rev. Lett.* 87 (2001) 215502.
- [10] Y. F. Gu and Y. F. Chen, *Phys. Rev. B* 76 (2007) 13411.
- [11] L. G. C. Rego and G. Kirczenow, *Phys. Rev. Lett.* 81 (1998) 232.
- [12] L. G. C. Rego and G. Kirczenow, *Phys. Rev. B* 59 (1999) 13080.
- [13] M. P. Blencowe, *Phys. Rev. B* 59 (1999) 4992.
- [14] D. E. Angelescu, M. C. Cross, and M. L. Roukes, *Superlatt. Microstruct.* 23 (1998) 673.
- [15] K. Schwab, E. A. Henriksen, J. M. Worlock, and M. L. Roukes, *Nature* 404 (2000) 974.
- [16] W. X. Li, K. Q. Chen, W. H. Duan, *et al.*, *Phys. Rev. B* 72 (2005) 045422.
- [17] W. X. Li, K. Q. Chen, W. H. Duan, *et al.*, *Appl. Phys. Lett.* 85 (2004) 822.
- [18] L. G. C. Rego and G. Kirczenow, *Phys. Rev. Lett.* 81 (1998) 232.
- [19] M. C. Cross and R. Lifshitz, *Phys. Rev. B* 64 (2001) 085324.
- [20] K. Q. Chen, X. H. Wang, and B. Y. Gu, *Phys. Rev. B* 61 (2000) 12075.
- [21] W. Q. Huang, K. Q. Chen, Z. Shuai, *et al.*, *Phys. Lett. A* 336 (2005) 245.